Functional Anatomy of Pointing and Grasping in Humans

Scott T. Grafton,[1,2] Andrew H. Fagg,[3] Roger P. Woods,[4] and Michael A. Arbib[3]

[1]USC PET Imaging Sciences Center, Department of Radiology, [2]Department of Neurology, and [3]Center for Neural Engineering, University of Southern California, Los Angeles, California 90033 and [4]Division of Brain Mapping, Department of Neurology, University of California at Los Angeles, Los Angeles, California 90024

The functional anatomy of reaching and grasping simple objects was determined in nine healthy subjects with positron emission tomography imaging of regional cerebral blood flow (rCBF). In a prehension (grasping) task, subjects reached and grasped illuminated cylindrical objects with their right hand. In a pointing task, subjects reached and pointed over the same targets. In a control condition subjects looked at the targets. Both movement tasks increased activity in a distributed set of cortical and subcortical sites: contralateral motor, premotor, ventral supplementary motor area (SMA), cingulate, superior parietal, and dorsal occipital cortex. Cortical areas including cuneate and dorsal occipital cortex were more extensively activated than ventral occipital or temporal pathways. The left parietal operculum (putative SII) was recruited during grasping but not pointing. Blood flow changes were individually localized with respect to local cortical anatomy using sulcal landmarks. Consistent anatomic landmarks from MRI scans could be identified to locate sensorimotor, ventral SMA, and SII blood flow increases. The time required to complete individual movements and the amount of movement made during imaging correlated positively with the magnitude of rCBF increases during grasping in the contralateral inferior sensorimotor, cingulate, and ipsilateral inferior temporal cortex, and bilateral anterior cerebellum. This functional-anatomic study defines a cortical system for "pragmatic" manipulation of simple neutral objects.

Prehension requires the integration of visual and somatosensory information into a coordinated motor plan for transporting the arm to a target while shaping the hand to match the target geometry. The different components of the behavior are well timed so that finger enclosure occurs at the proper moment (Jeannerod, 1984). Kinematic studies employing a variety of perturbation algorithms have established the close interrelationship of transport and hand shaping (Marteniuk et al., 1990; Paulignan et al., 1990, 1991a,b; Gentilluci et al., 1991). The results suggest a modular organization to the neural systems controlling this type of movement (Jeannerod and Marteniuk, 1992).

The areas of the human brain that control prehension are not defined in detail. Patients with focal lesions primarily effecting prehension are rare (Jeannerod, 1988; Jeannerod et al., 1994). Lesions are most commonly centered in the posterior parietal lobe. Until recently, functional imaging studies have not examined visually guided reaching and grasping movements. Thus, the extent of cortical areas normally recruited in this task remains uncertain. Converging evidence from neural recordings in nonhuman primates suggests that the control of reaching and grasping is dispersed across multiple cortical domains (see reviews in Wise and Desimone, 1988; Kalaska and Crammond, 1992). Areas that contribute to the control of prehension include sensorimotor, premotor, parietal, and cerebellar areas. A direct correlation between human and nonhuman primate localization in relevant premotor and parietal cortex remains largely speculative given the many differences of cortical anatomy between species.

The question of where reach and grasp are controlled in humans motivated the following positron emission tomography (PET) experiment. Images of regional cerebral blood flow (rCBF) were acquired to define local synaptic activity during visually guided movements of the right arm. The tasks were designed to examine three issues: (1) to localize movement-related activity during reach and grasp or reach and point compared to eye movements; simple cylinders were used as targets to examine a "pragmatic" type of prehension; (2) to identify differences of rCBF responses during reaching with grasp and reaching with pointing movements; such a difference might identify areas that are recruited when prehension involves object manipulation; and (3) to determine if blood flow responses in cerebral cortex correlate with simple kinematic measurements obtained during the grasp task.

Materials and Methods

Subjects

Nine subjects participated in the study after informed consent was obtained in accordance with the Institutional Review Board of the University of Southern California. All were normal by medical interview and detailed neurologic examination. Their mean age was 24 (range 19–43) and the male:female proportion was 7:2. All were right handed as determined with a standardized inventory (Raczkowski and Kalat, 1980).

Behavioral Tasks

Subjects lay supine in the PET scanner with their head immobilized with a foam head restraint (Smithers Corp., Akron, OH). They performed three visually guided motor paradigms during PET imaging: grasp, point, and control. In the grasp task, subjects reached and grasped cylindrical targets repetitively for the duration of the 90 second PET scan. The targets were five Plexiglas dowels of length 14 cm, aligned vertically in a row and located 14 cm apart from each other. Each dowel was a different diameter: 90, 30, 48, 5, and 24 mm (from subject's left to right). The array was positioned over the subject at an optimal distance so that all targets could be easily grasped with the arm near full extension. Independent light sources were mounted within each dowel to specify which target should be grasped on each trial. Target illumination was controlled remotely by computer. Subjects were instructed to rest their right hand on their chest until one of the targets was illuminated. Then, they were told to reach and grasp the sides of the illuminated dowel using a precision grasp, "as if the dowel were an egg or a delicate object." As soon as they had made contact with the object, they were to return to the starting position with the hand resting on the chest. This starting position could be located anywhere on the chest, and there was considerable trial-to-trial variability in the starting location. As shown in Figure 1, the starting point variability was random and did not contribute to any of the subsequent analysis. One of the five targets was illuminated every 3 sec and remained illuminated for 1.5 sec. The first target appeared 9 sec after the start of tracer injection and scanning. Twenty-seven trials were presented per scan. Targets appeared in random order across all trials.

In the point task, the same target array was used. Subjects were instructed to point over the top of the dowels with their right hand using a natural pointing hand position with the index finger extended and all others flexed in a comfortable fist. As in the grasp task, they returned the hand to a resting position on the chest after each trial. Targets were presented at the same frequency and in random order.

Cerebral Cortex Mar/Apr 1996;6:226–237; 1047-3211/96/$4.00

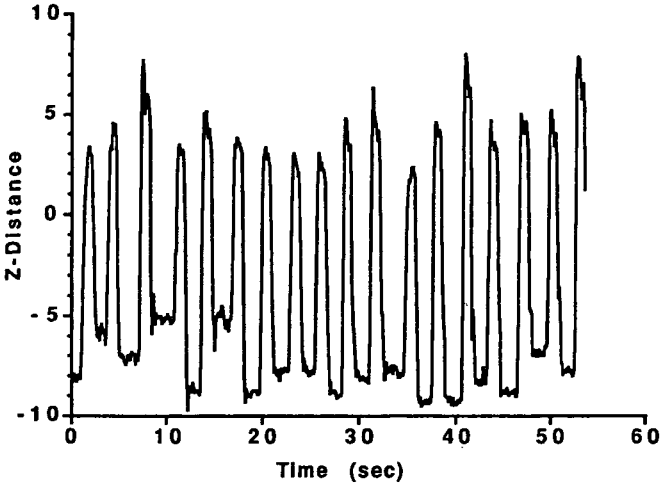

Figure 1. Arm movements during prehension. A tracking device, applied to the dorsum of the wrist, was used to map changes in the location of the hand as a function of time. Only relative changes of position are shown. Each trial began with the hand at rest on the chest (start position) followed by reaching movements and a grasp of different objects (targets). Z-distance values are uncalibrated units of distance along an axis parallel to the subjects supine body. The overall dwell time during which no movements were occurring during scanning could be measured from the flat portions of the plot. Subjects were allowed to vary the starting position from trial to trial, to make the returning movements more automatic. This explains the random differences in the z-position of the flat sections of the figure. The average time to complete one trial could also be measured. Because of limitations in the sampling frequency of the tracking device, velocity and acceleration profiles were not calculated.

For both point and grasp tasks, if subjects missed an illuminated target and did not perform a trial, they were told to simply wait for the next target and continue with the next appropriate movement. Ambient room light was present in all tasks and subjects could see the hand moving during the grasp and point tasks.

In the control task, subjects were told to leave the right hand at rest on the chest and to simply look at each target as it was illuminated. Subjects were not given a central fixation point between trials, since fixation was not used in the other two tasks. Instead, they were allowed to scan the targets in expectation of the next possible target similar to the point and grasp tasks.

Subjects practiced the tasks for 5 min prior to the first PET scan. Each set of three tasks was performed in random order, repeated three times (with new randomization) to minimize time-task interactions for a total of nine scans obtained in 90 min.

Performance Measures

The relative hand position was measured with a Polhemus tracking device (Polhemus, Colchester, VT). A transmitter was taped to the dorsum of the subject's right hand and an antenna was located near the targets. The device samples the three orthogonal coordinates and three axes of rotation relative to the remote antenna at a frequency of 10 Hz. Data were collected for only the first 18 trials of each scan because of computer memory limitations.

Absolute spatial calibration of the tracking device was unreliable due to electromagnetic field distortions secondary to the PET detector array and gantry. Therefore, only uncalibrated data were analyzed. Plots of spatial location versus time were graphically analyzed to determine the number of completed movement cycles, the total amount of movement time, the total amount of dwell time (time the hand was resting on the chest), and the duty cycle time (average time to complete one reach movement including the return to the starting position) during each scan. Because the Polhemus was limited to 10 Hz sampling and cannot be spatially calibrated near the scanner, more refined measures such as velocity or acceleration profiles were not derived.

Imaging

Images of rCBF were acquired using a modified autoradiographic method (Herscovitch et al., 1983; Raichle et al., 1983). For each scan, a bolus of 50 mCi of $H_2{}^{15}O$ was injected intravenously commensurate with the start of scanning and the behavioral task. A 90 sec scan was acquired and reconstructed using calculated attenuation correction, with boundaries derived from each emission scan sinogram. Arterial blood samples were not obtained. Images of radioactive counts were used to estimate rCBF as described previously (Fox et al., 1984; Mazziotta et al., 1985).

PET images of rCBF were acquired with the Siemens 953/A tomograph. The device collects 31 contiguous planes covering a 105 mm field of view. The nominal axial resolution is 4.3 mm at full width half-maximum (FWHM) and the transaxial resolution is 5.5 mm FWHM as measured with a line source. The tomograph was oriented 15° steeper than the canthomeatal line, so the field of view did not include the orbitofrontal cortex.

MRI images of anatomy were obtained with a GE Signa 1.5 T device. A three-dimensional volumetric gradient echo (SPGR) image of 124 contiguous slices (voxel size = 0.82 × 0.82 × 1.4 mm) was acquired using the sequence: TE = 5, TR = 21, flip angle = 45°). This sequence yields excellent anatomic detail and clearly differentiates gray and white matter.

Image Analysis

Image processing was performed on a SUN 10/41 SPARC workstation. The statistical image analysis required all rCBF images to be aligned in a common stereotactic reference frame. This transformation was accomplished in three steps. First, a within subject alignment of PET scans was performed using an automated registration algorithm (Woods et al., 1992). A mean image of the registered and resliced images was calculated for each subject. In the second step, the mean PET image from each individual was co-registered to the same subject's three-dimensional volumetric MRI scan using another automated algorithm (Woods et al., 1993b). This fit is also highly accurate, to within approximately 1.5 mm. In the third step, MRI scans from the different individuals were co-registered to a reference atlas centered in Talairach coordinates using an affine transformation with 12 degrees of freedom (Talairach and Tournoux, 1988; Woods et al., 1993a; Grafton et al., 1994). The parameters to be fit were three translations, three rotations, and three rescalers oriented in a direction specified by the last three parameters. This method provides a direct fit of MRI scans from different subjects to each other rather than to an idealized atlas or population based composite atlas. In addition, the method uses all of the MRI signal information to perform the fitting instead of a surface contour or a limited set of internal or external landmarks. The co-registered MRI scans were combined as a mean image to generate a population specific anatomic atlas centered in Talairach coordinates. The accuracy of the affine transformation for preserving the landmarks of the Talairach space has been tested previously in a separate validation experiment of eight subjects (Grafton et al., 1994). From the co-registered MRIs, each anterior-posterior commissural line was identified directly on sagittal, coronal, and axial images. The absolute group mean errors of the pitch angle was 1.6° relative to the atlas. The absolute group mean errors of the roll and yaw angles were less than 0.5°. The anterior commissure of each subject was identified and the absolute group mean error found to be 1.43 mm along the x-direction, 0.61 mm along the y-direction, and 1.85 mm along the z-direction relative to the atlas. Thus, the direct fitting approach preserves the nominal landmarks of the Talairach space.

Once the MRI scans were co-registered, the transformation matrices were applied to appropriate PET images so that rCBF images would also be centered in Talairach coordinates. To reduce the errors secondary to repeatedly reslicing and interpolating each of the PET images, all of the sequential reslice matrices for each scan were combined and a single transformation from each of the raw PET scans to the final image format in stereotactic space was calculated. PET blood flow changes were localized in an orthogonal reference frame as defined by the Talairach stereotactic space (Talairach and Tournoux, 1988). In one of the subjects, an MRI scan was not available. Mean PET images from this subject were matched to the mean PET images of the other subjects with the same affine transformation algorithm. Identification of the anterior-posterior commissural line and anterior commissure coordinates on the mean PET image after transformation confirmed that this subject was also accurately positioned in Talairach coordinate space (Minoshima et al., 1993).

Three-dimensional representations of the MRI data were generated with the AVS software package (Advanced Visualization Systems,

Table 1
Localization of task-related differences of rCBF

Anatomic location	Talairach coordinates (mm)			Mean rCBF (ml/min/100 gm)			ANOVA task main effect		Task comparisons: Movement − Control		Task comparisons: Grasp − Point	
	x	y	z	Control	Grasp	Point	F	p	Difference	CI	Difference	CI
L Premotor	−25	−22	64	50.2 (3.3)	55.4 (3.7)	55.1 (3.5)	15.5	0.00001	**5.0 (1.0)**	2.7 to 7.3	0.2 (0.8)	−1.7 to 2.1
R Premotor	27	−22	64	51.2 (2.8)	54.7 (4.6)	53.6 (5.1)	10.4	0.0005	**3.0 (1.0)**	0.6 to 5.5	1.1 (0.8)	−0.9 to 3.1
L Superior parietal	−33	−41	55	54.0 (5.5)	60.6 (2.5)	60.4 (3.4)	33.7	0.0000001	**6.5 (1.2)**	3.6 to 9.4	0.3 (1.0)	−2.1 to 2.6
R Superior parietal	33	−43	60	48.5 (6.1)	50.9 (5.7)	51.2 (5.8)	10.7	0.0005	**2.5 (0.7)**	0.9 to 4.1	−0.3 (0.5)	−1.6 to 1.0
L Sensorimotor	−30	−33	55	52.0 (2.2)	60.0 (3.9)	59.5 (3.3)	36.8	0.0000001	**7.7 (1.3)**	4.5 to 11.0	0.5 (1.1)	−2.1 to 3.1
R Sensorimotor	25	−27	56	50.0 (2.4)	52.7 (3.6)	52.6 (3.8)	14.1	0.00005	**2.7 (0.9)**	0.5 to 4.9	0.1 (0.8)	−1.7 to 1.9
L Cingulate	−6	−25	49	56.5 (4.7)	60.5 (3.9)	60.1 (4.0)	10.9	0.0005	**3.8 (0.9)**	1.5 to 6.0	0.4 (0.8)	−1.5 to 2.2
R Cingulate	8	−19	41	56.7 (5.6)	59.1 (6.5)	59.0 (5.0)	14.2	0.00005	**2.4 (0.9)**	0.1 to 4.6	0.1 (0.8)	−1.7 to 2.0
L Supplementary motor area	−1	−22	56	59.9 (2.7)	63.2 (3.1)	63.6 (2.8)	16.8	0.000005	**3.5 (1.0)**	1.1 to 5.8	−0.4 (0.8)	−2.3 to 1.5
L Parietal operculum	−36	−28	20	54.2 (8.0)	57.7 (7.6)	56.8 (6.3)	11.0	0.0005	**3.1 (1.0)**	0.8 to 5.4	1.0 (0.8)	−0.9 to 2.9
L Lateral parietal operculum	−53	−27	16	64.6 (2.7)	67.1 (2.1)	65.2 (2.2)	10.3	0.0005	1.6 (0.7)	−0.1 to 3.3	**1.9 (0.6)**	0.6 to 3.3
R Posterior parietal	17	−66	36	53.1 (3.4)	53.9 (3.0)	55.0 (3.2)	10.4	0.0005	1.4 (0.7)	−0.2 to 3.1	−1.1 (0.6)	−2.4 to 0.2
L Cuneate	−8	−95	4	52.6 (6.0)	56.3 (4.2)	55.3 (4.8)	11.0	0.0005	**3.2 (0.9)**	1.0 to 5.3	1.0 (0.7)	−0.8 to 2.8
R Cuneate	3	−77	23	64.1 (3.5)	67.3 (2.7)	67.2 (2.2)	13.2	0.00005	**3.2 (1.0)**	0.8 to 5.5	0.1 (0.8)	−1.8 to 2.0
L Dorsal occipital	−15	−88	20	51.2 (5.0)	54.4 (4.9)	54.3 (4.4)	10.9	0.0005	**3.2 (0.8)**	1.4 to 5.0	0.1 (0.6)	−1.4 to 1.6
L Inferior occipital	−33	−81	−9	49.0 (4.2)	50.7 (3.4)	51.0 (3.6)	10.3	0.0005	**1.9 (0.7)**	0.3 to 3.4	−0.3 (0.5)	−1.6 to 1.0
R Inferior temporal	41	−74	−1	47.2 (2.6)	49.4 (2.5)	48.4 (3.5)	11.3	0.0001	1.7 (0.7)	−0.1 to 3.4	1.1 (0.6)	−0.4 to 2.5
L Pulvinar thalamus	−19	−28	9	52.9 (3.9)	55.2 (4.4)	54.3 (4.3)	10.1	0.0005	1.8 (1.0)	−0.5 to 4.2	0.9 (0.8)	−1.0 to 2.8
L Ventrolat. thalamus	−12	−8	4	51.1 (3.2)	53.7 (3.4)	52.4 (2.9)	11.0	0.0005	1.9 (1.0)	−0.5 to 4.4	1.3 (0.8)	−0.7 to 3.3
R Cerebellar vermis	0	−57	−16	57.8 (4.0)	64.1 (4.6)	62.9 (4.7)	44.5	0.0000001	**5.7 (1.1)**	3.1 to 8.3	1.3 (0.9)	−0.8 to 3.4
R Anterior cerebellum	12	−41	−20	55.6 (2.8)	61.9 (4.9)	61.4 (6.1)	39.9	0.0000001	**6.1 (1.2)**	3.1 to 9.0	0.5 (1.0)	−1.9 to 2.9
L Anterior cerebellum	−20	−43	−23	56.1 (2.8)	61.3 (3.2)	60.2 (3.3)	29.5	0.0000001	**4.6 (0.9)**	2.4 to 6.8	1.1 (0.8)	−0.7 to 2.9

All locations are reported relative to Talairach stereotactic coordinates (Talairach and Tournoux, 1988). Mean rCBF values for the three tasks and standard deviation (in parentheses) are shown. Significant task differences were determined by a three-way ANOVA, randomized block design. An omnibus test, adjusted for the number of resolving elements (183), used a critical threshold of $F = 9.26$, $p < 0.000362$ (df, 2, 52). The maximum F and corresponding p value for each site reaching significance are shown. Task comparisons were further evaluated by two planned comparisons of means with linear contrasts. Movement − Control is the mean of the grasping and pointing tasks versus the control task. Grasp − Point is the difference of the two movement tasks. Mean contrast differences and standard deviations (in parentheses) are shown. To facilitate comparison with future PET studies, the 95% confidence intervals (CI) of the task differences (after adjusting for multiple comparisons of treatment effects) are also shown. Significant differences identified by this post hoc Bonferroni procedure are in boldface.

Waltham, MA). A mean MRI image of all subjects was also calculated. The resultant cortical rendering represents an average of all the MRI studies. As shown in later figures, gyral and sulcal anatomy with little spatial variance across subjects can be readily identified. Examples include the central sulcus, the intraparietal sulcus, and the superior frontal gyrus. Tertiary gyri with high spatial variance cannot be distinguished on the cortical representation. PET statistical results were then superimposed onto the three-dimensional rendering to localize rCBF changes with respect to the cortical surface.

Statistical Tests

PET rCBF images were masked below a 10% (of maximum) threshold and areas above this cutoff were smoothed to a final isotropic resolution of 20 mm full width half-maximum (as verified with a line source). Previous investigations demonstrate this magnitude of smoothing enhances signal detection (Grafton et al., 1990; Friston et al., 1991; Worsley et al., 1992).

After stereotactic co-registration, a mask consisting of all pixels for which data was available from all 81 PET scans was generated. For the given degree of image smoothing, the volume of this mask yielded approximately 138 gray matter resolving elements (Worsley et al., 1992).

All 81 smoothed images were normalized to each other using proportionate scaling calculated from the global activity of each scan. Normalization was performed using the common volume mask defined above, to avoid global normalization errors associated with missing data.

A three-way analysis of variance (ANOVA) was used to identify significant task effects (Neter et al., 1990). The three effects (and sources of variance) in the statistical model were task, repetition, and subject. To account for the intersubject subject variance, a randomized blocking design was used with subjects as a blocking effect. This model formally incorporates the extra information that is available in an experimental paradigm where each of the tasks is performed more than once, and in which each subject performs all the tasks and repeats. In addition to the usual assumptions of normality inherent in ANOVA, the three-way ANOVA model we used requires no three-way task-subject-repetition interactions. Given the nature of the behavioral paradigm under investigation, this is a reasonable assumption. Before calculating a final test statistic, we ruled out the presence of significant task-subject and task-time interactions. Neither of these interactions were significant at any pixel. The final three-way ANOVA model allows for time-subject interactions. An F map image of significant task effects was calculated on a pixel by pixel basis (df = 2, 52) and a threshold was set for $F = 9.26, p < 0.000362$. This amounts to a strict Bonferroni correction for approximately 138 resolving elements. Peak sites on the F map above this threshold were localized and maximal F and p values and mean rCBF values were tabulated. The resultant F test calculates main task effects but it does not identify which of the behaviors are significantly different from the others. A post hoc Bonferroni test ($p < 0.05$ after correcting for multiple comparisons) was used to identify significant differences between movement (grasp and point) versus control and type of movement (grasp vs point). Task differences are reported in

→

Figure 2. Task-related differences of rCBF. All pixels in which there was a significant difference between the three tasks (grasp, point, control) are shown in yellow ($p < 0.001$). These differences are superimposed on an anatomic reference image derived from the mean of the individual's MRI scans. The anatomic reference discloses primary and secondary sulci despite the intersubject averaging of MRI's after the images were transformed into Talairach coordinates. *A*, Superior view (frontal lobes on image left). The *arrow* shows the location of the ventral SMA and adjacent cingulate cortex, which were increased in activity for both pointing and grasping tasks relative to control. Both sites are caudal to the anterior commissure. Also visible are bilateral flow changes in sensorimotor, premotor, and parietal cortex. *B*, Posterior view (left hemisphere on image left). The *upper arrow* points to a conglomerate of posterior parietal and dorsal occipital flow changes that were increased in activity for both the pointing and grasping tasks relative to control. The increased activity extended into parasagittal bilateral cuneate cortex. More extensive differences are present in left than right hemisphere. The *lower arrow* points to movement-related flow

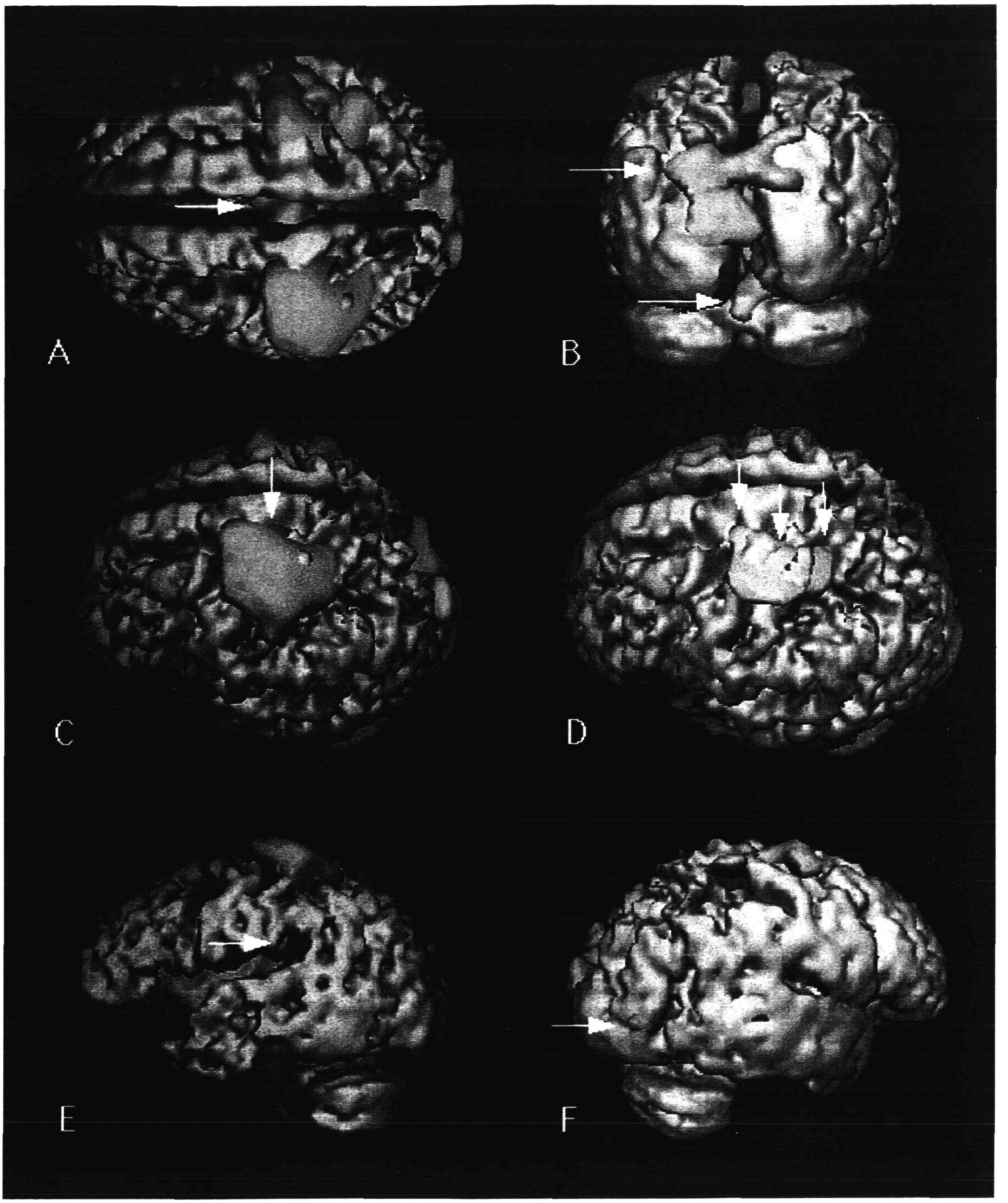

changes in bilateral anterior cerebellum and vermis. *C,* Left superior oblique view (frontal lobe on image left). *Arrow* points to three contiguous changes of blood flow located in premotor, sensorimotor, and parietal cortex contralateral to the moving limb. *D,* Same view as *C* with statistical threshold increased to $p < 0.00005$ to demonstrate the three sites with maximal changes of rCBF. The *three arrows* point to flow differences in left premotor, sensorimotor, and parietal cortex. In the correlation studies of rCBF and kinematics, the inferior aspect of the blood flow change in sensorimotor cortex showed the closest correlation to movement parameters. *E,* Left lateral view (frontal lobe on image left). Location of parietal operculum activity. This blood flow response was significantly greater during grasp than pointing. The site is located in the putative area of SII. *F,* Right posterior oblique view (occipital lobe on image left). *Arrow* points to location of right inferior temporal cortex flow increase. Note the minimal extent of rCBF increases in ventral occipital and temporal areas compared with dorsal areas shown in *B.*

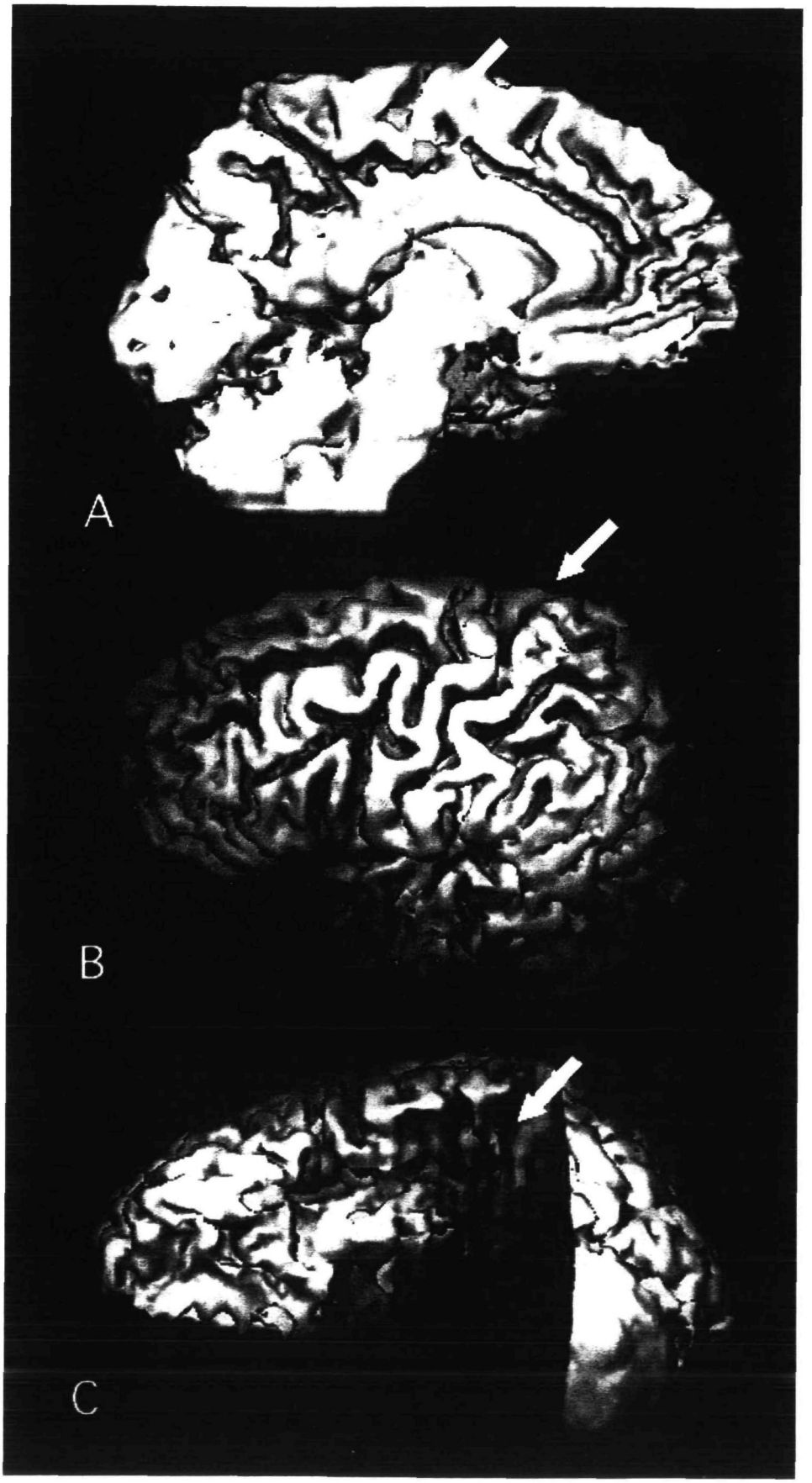

Figure 3. Three-dimensional localization of cortical blood flow increases in a single subject. Standardized views were created of the mesial surface of the left hemisphere (*A*), superior oblique views of the lateral surface of the left hemisphere (*B*,) and inferior oblique views of the parietal operculum after the temporal lobe has been removed to facilitate visualization of the opercular cortex (*C*). Major sulci were traced and flow changes initially identified by the group analysis were localized in each individual with respect to sulcal landmarks (*arrows*).

95% confidence intervals to facilitate future comparison with other studies.

Individual subject localization was determined by calculating a percent change of rCBF between the three grasp tasks and the three control tasks. Changes greater than 10% were superimposed on the same subject's MRI scan and rendered in three dimensions using AVS. Standardized views (30° left superior oblique, 60° left inferior oblique, and right lateral of left mesial cortex) were saved as PICT files. Local sulci and rCBF increases were traced using Adobe ILLUSTRATOR on a Macintosh PowerPC. Sulci were named using the conventions of Ono et al. (1990).

Correlation Analysis

A correlation was made between kinematic measurements and changes of rCBF. The three grasp and three control rCBF scans were average together and a percent change of rCBF image was calculated for each subject. Each of the kinematic parameters (also in triplicate) also were averaged together, yielding one of each measurement per subject. Then, a Pearson correlation between change of rCBF (grasp vs control) and each kinematic parameter was calculated on a pixel by pixel basis with a threshold of $p < 0.01$. This would identify, for example, areas where rCBF increases are of a greater magnitude in subjects who move for a longer period of time compared to those who move for a short time. To reduce the number of repeat correlations, only pixels shown to have significant task effects by the three-way ANOVA were correlated with movement parameters. Significant sites were graphically evaluated to confirm that the correlation was not due to outliers.

Results

Movement parameters

A plot of one subject's tracking movements as a function of time is shown in Figure 1. Each reach and grasp cycle is readily distinguished from the baseline intertrial resting position. The performance data obtained with the hand tracking apparatus revealed that subjects took slightly longer to complete each grasping movement (1.87 ± 0.10 sec/cycle) than pointing movement (1.69 ± 0.06 sec/cycle) ($t = 3.05, p < 0.01$). This is consistent with previous kinematic studies of reaching tasks with and without grasping (Marteniuk et al., 1987). Although they took longer to complete the grasp task, subjects were also more likely to miss one of the targets in the grasp, culminating in less completed movement cycles in the grasp task (15.7 ± 1.5 of 18 completed trials) compared to the pointing task (16.8 ± 0.1 of 18 completed trials) ($t = 3.64, p < 0.01$). The missed trial occurred randomly and with any of the targets. The two measurements, time to complete a movement cycle and total number of movements counterbalanced each other so that the total fraction of time during imaging with limb movement (or its inverse, the total dwell time) was not significantly different for grasping (59% ± 9) and pointing tasks (57% ± 8). Thus, any differences in the grasp and point tasks could not be ascribed to differences in the total amount of movement made during scanning.

Imaging Studies

All cerebral areas showing significant task differences are summarized in Table 1. Although the threshold for detection was set for a probability of $p < 0.000362$, it is obvious from Table 1 that in most locations the p-values were orders of magnitude smaller, supporting the certainty of the statistical results irrespective of the problem of false positives arising from multiple comparisons.

The task-related differences were present in a widely distributed set of areas involving cortex, thalamus and cerebellum. The location of the cortical sites with respect to local gyral anatomy of the groups average brain morphology are shown in Figure 2. Significant task effects are located in three cortical domains. One set of changes are located in primary sensorimotor cortex and nearby premotor and superior parietal cortex. A second set is located in the mesial frontal cortex, with flow changes in the ventral and caudal aspect of the supplementary motor area (SMA). This site is caudal to the vertical axis of the anterior commissure and rostral to the mesial portion of the motor cortex. Changes are also present in the nearby cingulate "motor" area. The third set of blood flow changes is located posteriorly, in bilateral dorsal occipital, posterior parietal and inferior temporal and occipital cortices. One interesting observation is the relative lack of task effects in frontal lobes. A second interesting feature is that the increases in posterior parietal and dorsal occipital lobes are very close to the midline and not in the intraparietal fissure. Instead, rCBF responses involve cuneate and adjacent parieto-occipital cortex. A third interesting feature is the two rCBF responses located in the parietal operculum, in a region considered to include the second somatosensory cortex (SII).

Mean rCBF values at each location and results of a post hoc Bonferroni comparison of the three tasks are also summarized in Table 1. As one might expect, the basis for the significant task effect was most frequently ascribed to differences between movement (grasp and point) and the control task. A direct comparison of the two movement tasks (grasp − point) revealed a significant difference in only one site, the left lateral parietal operculum. For several sites the basis for the significant difference was not significant using the post hoc method. Examination of the task means reveals the source of the differences. The right inferior temporal cortex, left pulvinar thalamus, and left ventrolateral thalamus were maximally activated during the grasp task, but the difference between grasp and point did not reach significance. The right posterior parietal cortex showed maximal rCBF differences with the control task but not with grasping. No sites were significantly greater during pointing than grasping.

Individual Subject Localization

Blood flow increases in the region of the sensorimotor cortex, in the mesial frontal cortex, and in the parietal operculum were localized in the eight individuals with co-registered MRI scans. An example of the three-dimensional topography for one subject is shown in Figure 3. Increases of rCBF > 10% are superimposed on the same subject's MRI scan. These three-dimensional views were used to trace the local sulcal anatomy using the naming conventions of Ono et al. (1990). Blood flow responses in proximity to the sites identified in Table 1 were then traced. Other changes of rCBF were not traced since they were not identified as significant in the group analysis.

Intersubject differences in the localization of rCBF responses with respect to sulcal anatomy are summarized in Figures 4–6. In Figure 4, the central sulcus and adjacent precentral and postcentral sulcus were identified directly from the three-dimensional MRI renderings. The superior frontal sulcus could also be reliably identified in all cases. Location of the intraparietal sulcus was less certain, consistent with the greater intersubject variability of this sulcus (Ono et al., 1990). A consistent blood flow increase can be located in the depth of the central sulcus, covering both primary sensory and motor cortex. In all cases, the increase is located near the genu of the central sulcus. In six of eight subjects a site can be detected in the premotor cortex rostral to the genu of the central sulcus. Most commonly it is located in the precentral sulcus dorsal to the superior frontal sulcus. There are several variations including localization to the sulcus ventral to the superior frontal sulcus and to the superficial cortex of the precentral gyrus. A third site is located in the postcentral sulcus in eight of eight subjects. Most commonly (seven of eight) it is located dorsal to the estimated intersection of the intra-

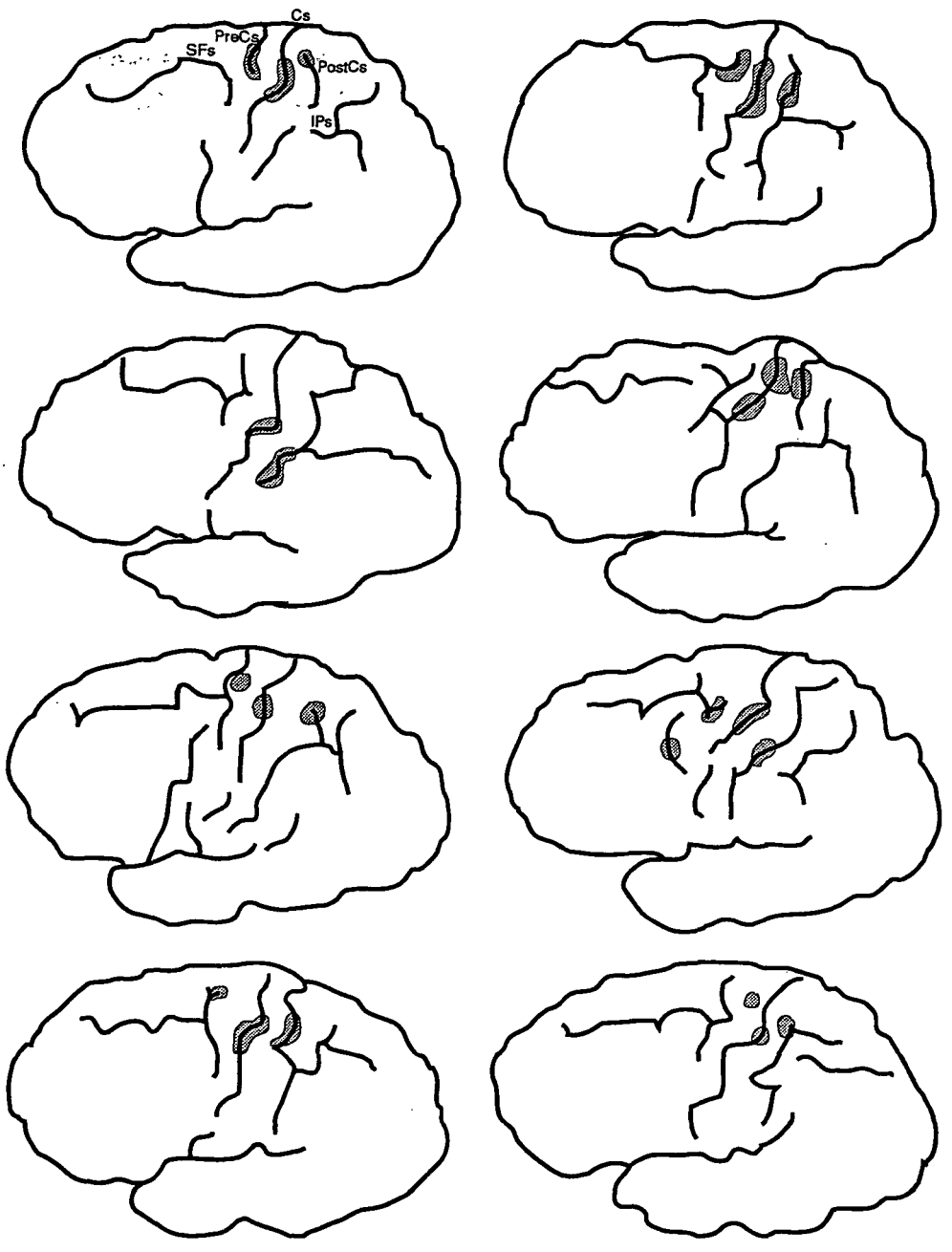

Figure 4. Localization of frontal and parietal blood flow increases during grasping task. Major sulci in the region of the central sulcus (*Cs*) were traced from left superior oblique three-dimensional images of the lateral surface of the brain. The central sulcus, superior frontal sulcus, (*SFs*), precentral sulcus (*PreCs*), and postcentral sulcus (*PostCs*) could be reliably identified in all cases. The intraparietal sulcus (*IPs*) was variable in location, orientation and point of intersection with the postcentral sulcus. In all subjects sensorimotor activity was present at the genu of the central sulcus. Premotor activity was close to the intersection of the superior frontal sulcus and precentral sulcus and located either in the depth of the precentral sulcus or superficially, on the convexity of the precentral gyrus. The postcentral flow increase was located dorsal to the intraparietal sulcus or its estimated intersection with postcentral sulcus in all but one subject.

parietal sulcus with the postcentral sulcus. In one subject it is ventral to the intersection.

Blood flow increases of the mesial frontal cortex are also consistent with respect to local sulcal anatomy. In eight of eight subjects a discrete flow response is present in the cingulate sulcus, in an area that presumably corresponds to the cingulate motor area observed in nonhuman primates (Luppino et al., 1991). In all cases the increase is in the caudal aspect of the cingulate sulcus, close to the paracentral sulcus. In six of eight subjects a second site is located in the paracentral lobule, dorsal to the cingulate sulcus in the putative SMA. Our landmarks for defining the boundaries of the human SMA are the cingulate sulcus (ventral), the boundary of the lateral surface of the hemisphere (dorsal), the vertical axis of the anterior commissure (rostral), and the extension of the central sulcus onto the mesial surface (caudal). The cortex extending caudal to the central sulcus boundary to the marginal ramus of the cingulate cortex is leg area of the primary motor cortex. This demarcation of human frontal cortex is supported by recent cytoarchitectonic studies (M. Matteli, personal communication). In this framework all six flow increases are located in the ventral-caudal aspect of the putative human SMA. Most commonly the flow response is located close to or within the paracentral sulcus. In the one subject with interruption and duplication of the cingulate sulcus in the area of the paracentral sulcus the SMA blood flow increase is located more rostrally (subject 5; Fig. 5).

In the group analysis two adjacent sites show significant task effects in the parietal operculum. The more lateral of these sites has a greater increase of flow during grasping than pointing. Intersubject differences in the location of these blood flow increases with respect to local sulcal anatomy are shown in Figure 6. In six of eight cases, the blood flow increases are located in the sulcus extending from the parietal

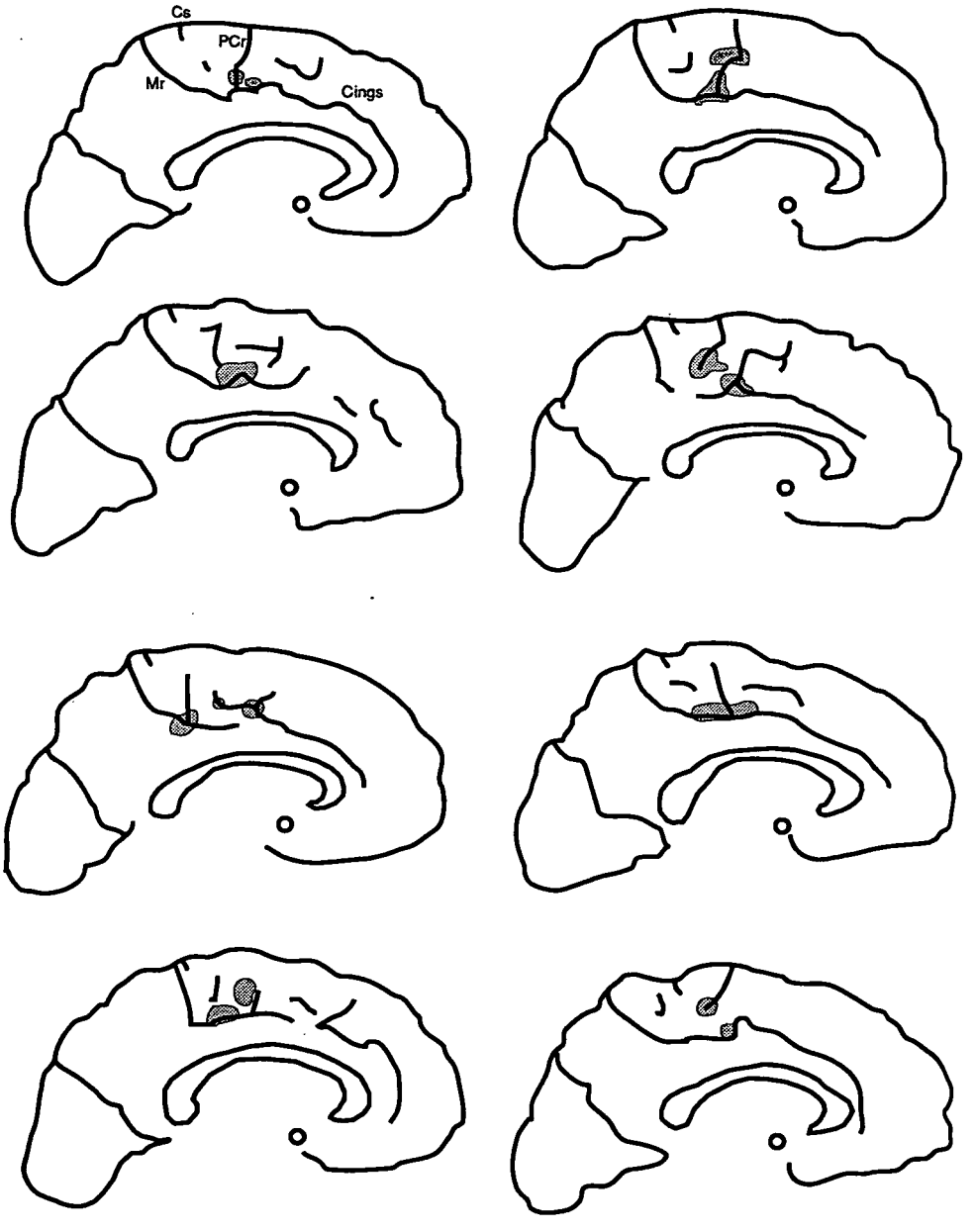

Figure 5. Localization of left mesial frontal blood flow increases during grasping task. Major sulci in the region of the left mesial cortex were traced from three-dimensional images after removing the right hemisphere. The anterior commissure is located at the location labeled with a circle. The cingulate sulcus (*Cings*) was continuous in 50% of subjects. Interruptions in the others were located both close to the marginal ramus (*Mr*) or more rostrally. A paracentral ramus (*PCr*) was present in all subjects. Increased activity could be identified in the putative motor area of the cingulate sulcus in eight of eight subjects. A second site was present in the paracentral lobule in six of eight subjects. This site was most commonly in the paracentral ramus in the ventral and caudal aspect of the putative SMA. Both sites were rostral to the central sulcus (*Cs*) and caudal to the anterior commissure.

operculum onto the lateral surface of the hemisphere (the posterior subcentral sulcus). The mesial site is most commonly (six of eight) located at the intersection of the posterior subcentral sulcus and the insular cortex. The results suggest that human SII is centered in the posterior subcentral sulcus.

rCBF Correlates of Performance

Five sites were identified where the magnitude of rCBF changes (grasp − control) correlated with simple kinematic measurements. The location of these sites are summarized in Table 2.

The correlations are located in contralateral sensorimotor and cingulate "motor" cortex, bilateral anterior cerebellum, and the ipsilateral inferior temporal cortex. The correlations were stronger for the transport time (average time required to reach out, grasp a target, and return to rest position) than for the percent movement time (the fraction of time during imaging when the hand was moving). Figure 7 shows the regression plots of the two kinematic measures with rCBF changes in these four sites.

Discussion

We have identified a distributed set of cortical areas that are activated during prehensile movements in humans. For nearly all of the sites, there is increased activity whether a subject is reaching and pointing toward or reaching and grasping simple cylindrical objects. With the implementation of individual subject analysis it is now possible to localize some of these blood flow changes with respect to local sulcal anatomy. Sensorimotor activations were typically at the genu of the central sulcus. This location for the arm and hand area has now been defined in three separate neuroimaging tasks (Grafton et al., 1991; Rumeau et al., 1994). Premotor blood flow increases were most commonly in the nearby precentral sulcus and near the superior frontal sulcus. The flow response is very close to the central sulcus and is potentially difficult to distinguish from the sensorimotor flow response, particularly with group averaging or excessive image smoothing. This dorsolateral premotor site has been mapped previously in tasks requiring both conditional and unconditional movement selection (Deiber et al., 1991; Petrides et al., 1993).

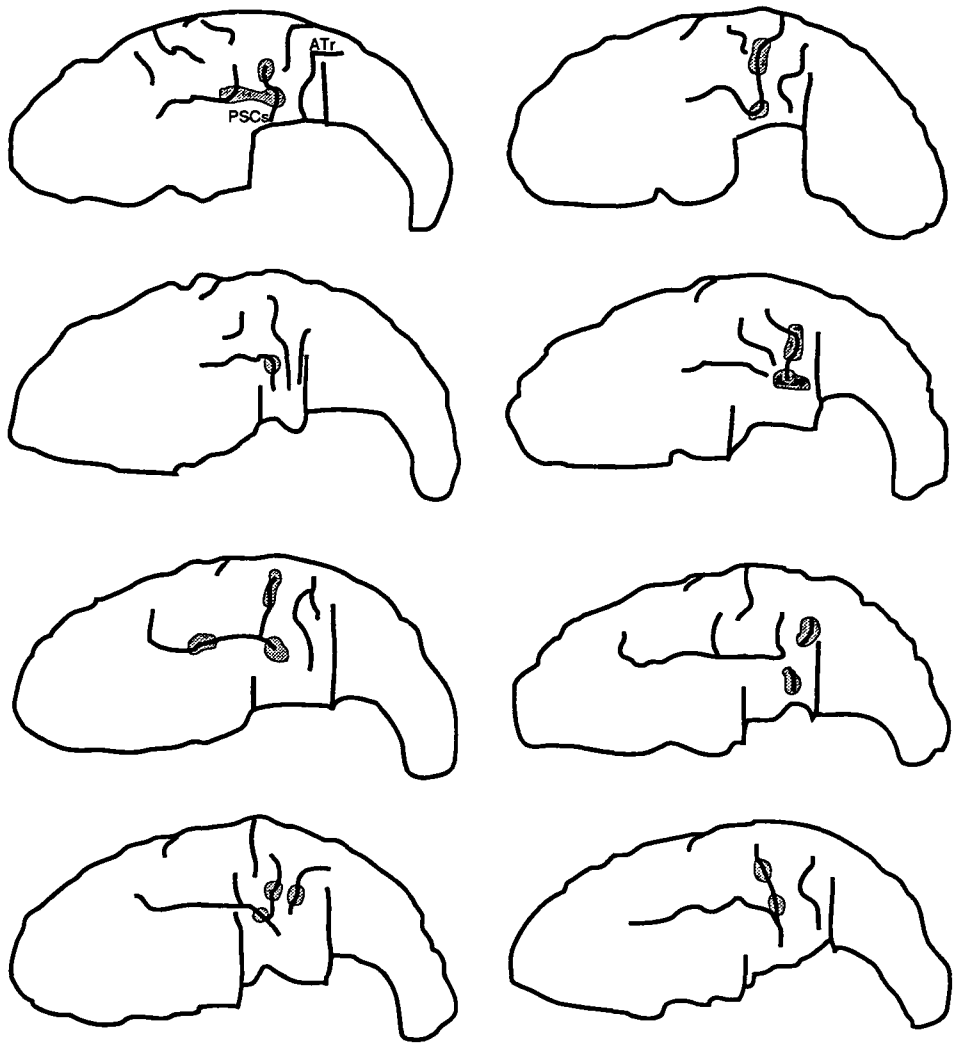

Figure 6. Localization of parietal operculum blood flow increases during grasping task. Major sulci in the region of the left parietal operculum were traced from left inferior oblique three-dimensional images. The anterior temporal lobe has been removed to facilitate examination of the opercular area. Two sites were most commonly observed in the operculum. The sites were usually located in the posterior subcentral sulcus (*PSCs*) and not the ascending terminal ramus (*ATr*) of the lateral fissure. The lateral of the two sites showed a significantly greater activation during grasping than pointing.

As in other PET investigations of visuomotor control, parietal flow increases were located in superior parietal cortex. In humans, unlike nonhuman primates, the parietal cortex superior to the intraparietal sulcus includes Brodmann's area 5 and 7 (Eidelberg and Galaburda, 1984; Mesulam, 1985; Talairach and Tournoux, 1988; Damasio and Damasio, 1989). The blood flow increase in this area was almost always in the postcentral sulcus and dorsal to the estimated intersection of the intraparietal sulcus with the postcentral sulcus, in what is accepted as Brodmann's area 7. Relative activity in superior parietal cortex is increased in other motor tasks, including drawing spirals in the air, tracking the fingers through a maze, movement selection and integrating visual information into a plan for intended movements (Roland et al., 1980; Deiber et al., 1991; Grafton et al., 1992). The common feature of these diverse tasks has been the process of visuomotor transformation in extrapersonal space.

Table 2
Correlation of movement-related changes of rCBF with performance measurements

	Talairach coordinates (mm)			rCBF – Movement correlation			
				Transport time		Percentage movement time	
Anatomic location	x	y	z	*r*	*p*	*r*	*p*
L Sensorimotor	−28	−25	46	0.845	0.008	0.801	0.017
L Cingulate	−9	−17	43	0.866	0.005	0.836	0.010
R Inferior temporal	36	−65	−3	0.882	0.004	0.875	0.004
L Anterior cerebellum	−25	−43	−21	0.810	0.015	0.860	0.006
R Anterior cerebellum	20	−39	−18	0.848	0.008	0.832	0.010

The percentage rCBF increase (grasp vs control) at each site was correlated with two movement measurements. All locations are reported relative to stereotactic atlas of Talairach and Tournoux (1988). Transport time is the average time required to reach, grasp a target object, and return to starting position. Percentage movement time is the fraction of time during a 90 sec PET scan when the hand and arm were moving.

Multiple sites in inferior temporal, posterior parietal, and dorsal occipital cortex were more active during the movement tasks. During the two visually guided tasks there was perception of visual motion of the arm and hand. These were compared to an eye movement control scan with no apparent movement. Thus, it is difficult to exclude the possibility that increased activity in these sites was simply related to motion detection. The right inferior temporal site in our study is located 7 mm anterior to a site previously identified as a possible human homolog of area MT (Kaas, 1992). The MT site demonstrates exquisite motion sensitivity (Zeki et al., 1991; Watson et al., 1993). Thus, we cannot suggest any additional functional attributes to this site besides motion detection with our protocol. More recently, Dupont et al. (1994) have defined additional motion sensitive cortex in humans using different visual stimuli. Again, a blood flow increase was de-

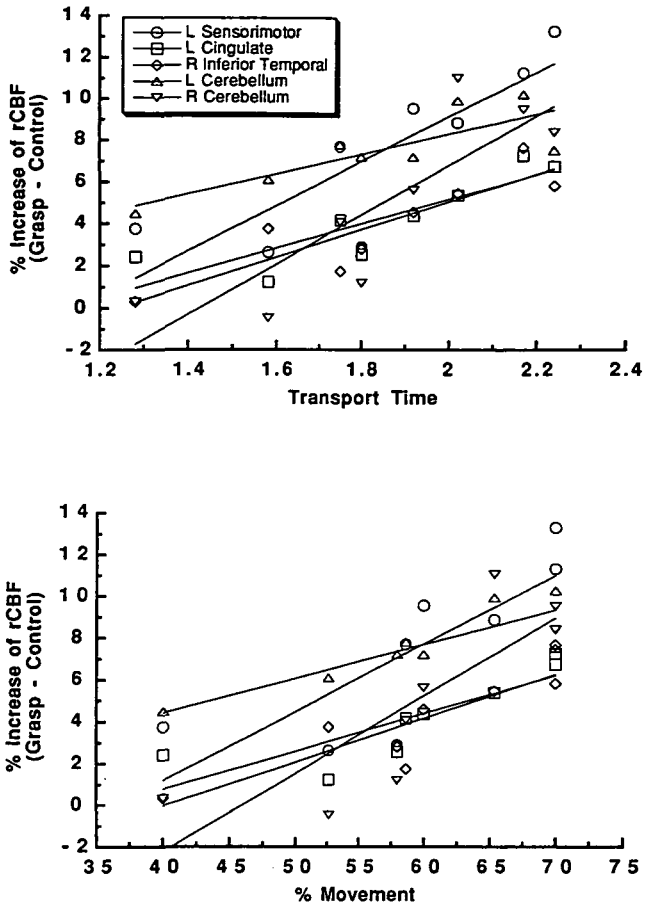

Figure 7. Correlation of rCBF increase and two kinematic parameters. Eight subjects were able to complete > 85% grasp movements during imaging and are included in this analysis. The percentage increase of rCBF (grasp vs control) was calculated for all pixels in which a significant movement effect was measured by ANOVA. At five sites the change of rCBF correlated with the Transport Time, that is, the average time required to complete each grasp movement ($p < 0.01$). These sites were located in the left sensorimotor cortex, left cingulate cortex, bilateral anterior cerebellum and right inferior temporal cortex. These correlations are shown in the *upper graph*. The change of rCBF in these areas also correlated with the percentage movement, that is, the percentage of time during scanning during which movements of the arm were occurring, but to a lesser degree. These correlations are shown in the *lower graph*.

tected in the MT site. Additional areas were located in the cuneate cortex and parieto-occipital fissure. However, the locations of these flow changes are less extensive in size and not centered near the findings in our study. Thus, it is possible that the increased activity dorsal occipital and posterior parietal cortex detected during reaching and grasping are involved in more than just motion detection. Recently, Decety and co-workers used a virtual reality visual display system to examine perception of a virtual hand moving toward a target compared to imagined and real movements (Decety et al., 1994). Again, the putative MT area showed simple motion sensitivity, but not the areas observed in posterior parietal cortex. Our results suggest that the posterior parietal cortex is involved in the control of directed limb movements toward simple objects, both with and without a grasp. The occipital and parietal cortex dorsal to the visual cortex is more extensively activated than inferior temporal or occipital pathways, consistent with the notion that a dorsal information stream is recruited in simple pragmatic reaching movements.

A related question is whether some of the changes in this study could be secondary to differences in the level of spatial attention used for each task. It is possible that subjects use more directed attention in tasks requiring limb movement (grasp or point task) than for the oculomotor control task. One argument against this possibility is the observation that the locations of increased blood flow in the present study (particularly in the parietal cortex) do not correspond to flow changes associated with spatial attention in a series of human PET experiments (Corbetta et al., 1990, 1993). Nevertheless, directed attention remains a "mandatory process" across tasks, and one that cannot always be fully controlled for in the PET imaging environment (Sergent, 1994).

The main difference between the grasp and point tasks was the marked activity in the parietal operculum during grasping, in a site containing the putative SII. This area is comprised of both simple sensory neurons with response properties similar to SI as well as complex sensory neurons. One interpretation of our data is that the increased SII activity is merely due to greater simple sensory input because the subjects are touching the objects in the grasp task and not in the point task. In recent PET studies this area shows activation similar to SI during simple somatosensory stimulation (Fox et al., 1987). This interpretation is probably not sufficient for our results, as the primary sensory cortex showed no difference in activity between the two tasks. Instead, we speculate that in prehension the parietal operculum is also involved in higher level processing of object shape based on tactile information. This is supported by anatomic, physiologic and lesion studies. SII receives projections from all portions of the primary sensory cortex: areas 3a, 3b, 1, and 2; SII projects to area 4. Using anatomic tracing methods, Friedman et al. (1986) found nonhuman primate SII to also be reciprocally connected with the retroinsular area, area 7b, and the granular and dysgranular insular fields. In detailed anatomical studies in the macaque, Preuss and Goldman-Rakic (1989) found an interconnected network of forelimb and orofacial representations involving the ventral premotor cortex (area 6v or F5), orbitofrontal opercular areas, the opercular portion of area 2, SII, the central insula and area 7b. Mishkin (1979) proposed that the strong coupling of SII and the posterior insula and limbic areas might provide a suitable architecture for tactile object learning. This would be analogous to the ventral pathway from occipital to temporal cortex used for visually based object recognition and learning. Ablation studies in nonhuman primates result in decrements of performance during tactile discrimination and impaired tactile learning, particularly when the lesion is placed contralateral to the preferred hand (Garcha and Ettlinger, 1978, 1980). Functional studies of this area in humans are rare. Penfield was the first to map this area with direct cortical stimulation (Penfield and Jasper, 1954; Lüders et al., 1985). Cortical stimulation in awake subjects typically causes simple sensory symptoms. Focal lesions of the parietal operculum characteristically produce tactile agnosia without loss of simple tactile sensation, or motor control (Caselli, 1991, 1993). This deficit can include the inability to sort objects based on size or shape, although sorting of texture is preserved. Further imaging studies in which the effect of simple somatosensory input is counterbalanced across tasks are required to further elucidate the role of SII in prehension tasks.

There were two important negative findings in this study. The first was a lack of increased activity in any ventral premotor area on either the lateral cortical surface or in the frontal operculum. It has been suggested that a site in this area might show flow changes during grasping tasks, based on nonhuman primate studies. For example, single unit recordings in nonhuman primates implicate ventral premotor areas such as 6v (F5) in the control of prehensile movements of the hands and mouth (Rizzolatti, 1987; Rizzolatti et al., 1987).

The only movement-related premotor area in our human study was located in dorsal area 6 (F2), near the superior frontal sulcus. We suspect that this site corresponds to dorsal premotor cortex in nonhuman primates; an area implicated in conditional motor learning as well as reach and grasp tasks (Mitz et al., 1991; di Pellegrino and Wise, 1993). The second negative finding was a lack of movement-related activity in the region of the intraparietal sulcus. Here too, there is evidence of single unit activity correlated with manipulation of objects (Taira et al., 1990; Sakata et al., 1992).

The negative PET findings in these two areas could be due to several possibilities. There may be interspecies differences in the organization of premotor or intraparietal cortex. For example, the expansion of human premotor cortex to include a Broca's area complicates comparison of the anatomy of ventral premotor cortex. Intersubject variability adds another dimension of uncertainty. The human intraparietal sulcus is variable in location and number of interruptions (Ono et al., 1990). This hinders intersubject comparisons and also reduces the likelihood of obtaining intersubject co-registration and statistical significance in this area. Third, there may be cases where neuronal activity does not induce measurable blood flow changes. Finally, the task that we used may not cause sufficient behavioral demands to activate these areas. The use of cylindrical target objects in our prehension makes the task a simple "pragmatic" task, requiring no working memory or need to represent the object at a symbolic level (Goodale et al., 1991; Jeannerod et al., 1994). In this setting only dorsal parietal pathways may be required. From this we predict that with the use of more complex and familiar objects there will be increased activity of intraparietal cortex and ventral premotor areas.

Movement Time

The simplified kinematic measurements obtained in the present experiments expose two important relationships. The magnitude of rCBF responses in motor effector areas, including the motor cortex and mesial frontal motor area, are sensitive to the amount of time it takes to complete intermittent movements and to the total amount of movement made during the period of image acquisition. These interactions were observed in a completely paced intermittent task. Despite the pacing, if subjects completed each movement cycle more slowly, the end result was greater amount of time spent controlling a movement and greater relative activity in sensorimotor and cingulate motor areas. The result has implications for the interpretation of previous PET motor data where the relative magnitude of rCBF responses in the above noted areas was an important consideration and in which intermittent tasks were performed. This effect will make studies of motor learning, functional recovery after brain injury, and population comparisons particularly difficult to interpret if the relative contributions of movement and rest are not accounted for. Potential solutions to this problem include the use of continuous motor tasks, paced ballistic motor tasks, rapid image acquisition using echo planar MRI or multivariate statistical approaches that can account for the contribution of dwell time.

Notes

This work was supported by U.S. Public Health Service Grants KS-08 NS01568 (S.T.G.) and KS-08 NS01646 (R.P.W.) and a Human Frontier Research Program grant (S.T.G., M.A.A.). We thank John C. Mazziotta of the University of California at Los Angeles for generous software support, Michael Clark of Apple Computer for use of the Polhemus device, Kenny Martinez for data analysis, and Steve Hailes for technical assistance.

Address correspondence to Scott T. Grafton M.D., Department of Neurology, HCC Suite 350, 1510 San Pablo Street, Los Angeles, CA 90033-4606.

References

Caselli RJ (1991) Rediscovering tactile agnosia. Mayo Clin Proc 66: 129–142.

Caselli RJ (1993) Ventrolateral and dorsomedial somatosensory association cortex damage produces distinct somesthetic syndromes in humans. Neurology 43:762–771.

Corbetta M, Miezin FM, Dobmeyer S, Shulman GL, Petersen SE (1990) Attentional modulation of neural processing of shape, color, and velocity in humans. Science 248:1556–1559.

Corbetta M, Miezen FM, Shulman GL, Petersen SE (1993) A PET study of visuospatial attention. J Neurosci 13:1202–1226.

Damasio H, Damasio AR (1989) Lesion analysis in neuropsychology. New York: Oxford UP.

Decety J, Perani D, Jeannerod M, Bettinardi V, Tadary B, Woods R, Mazziotta JC, Fazio F (1994) Mapping motor representations with PET. Nature 371:600–602.

Deiber M-P, Passingham RE, Colebatch JG, Friston KJ, Nixon PD, Frackowiak RSJ (1991) Cortical areas and the selection of movement: a study with PET. Exp Brain Res 84:393–402.

di Pellegrino G, Wise SP (1993) Visuospatial versus visuomotor activity in the premotor and prefrontal cortex of a primate. J Neurosci 13:1227–1243.

Dupont P, Orban GA, DeBruyn B, Verbruggen A, Mortelmans L (1994) Many areas in the human brain respond to visual motion. J Neurophysiol 72:1420–1424.

Eidelberg D, Galaburda AM (1984) Inferior parietal lobule. Divergent architectonic asymmetries in human brain. Arch Neurol 41:843–852.

Fox PT, Mintun MA, Raichle ME, Herscovitch P (1984) A non-invasive approach to quantitative functional brain mapping with $H_2{}^{15}O$ and positron emission tomography. J Cereb Blood Flow Metab 4:329–333.

Fox PT, Burton H, Raichle ME (1987) Mapping human somatosensory cortex with positron emission tomography. J Neurosurg 67: 34–43.

Friedman DP, Murray EA, O'Neill JB, Mishkin M (1986) Cortical connections off the somatosensory fields of the lateral sulcus of macaques: evidence for a corticolimbic pathway for touch. J Comp Neurol 252:323–347.

Friston KJ, Frith CD, Liddle PF, Frackowiak RSJ (1991) Comparing functional (PET) images: the assessment of significant change. J Cereb Blood Flow Metab 11:690–699.

Garcha HS, Ettlinger G (1978) The effects of unilateral or bilateral removals of the second somatosensory cortex (area SII): a profound tactile disorder in monkeys. Cortex 14:319–326.

Garcha HS, Ettlinger G (1980) Tactile discrimination learning in the monkey: the effects of unilateral or bilateral removals of the second somatosensory cortex (area SII). Cortex 16:397–412.

Gentilluci M, Castiello U, Corradini ML, Scarpa M, Umiltá C, Rizzolatti G (1991) Influence of different types of grasping on the transport component of prehension movements. Neuropsychologia 29: 361–378.

Goodale MA, Milner AD, Jakobson LS, Carey DP (1991) A neurological dissociation between perceiving objects and grasping them. Nature 349:154–156.

Grafton ST, Huang SC, Mahoney DK, Mazziotta JC, Phelps ME (1990) Analysis of optimal reconstruction filters for maximizing signal to noise ratios in PET cerebral blood flow studies. J Nucl Med 31: 865.

Grafton ST, Woods RP, Mazziotta JC, Phelps ME (1991) Somatotopic mapping of the primary motor cortex in man: activation studies with cerebral blood flow and PET. J Neurophysiol 66:735–743.

Grafton ST, Mazziotta JC, Woods RP, Phelps ME (1992) Human functional anatomy of visually guided finger movements. Brain 115: 565–587.

Grafton ST, Woods RP, Tyszka JM (1994) Functional imaging of procedural motor learning: relating cerebral blood flow with individual subject performance. Hum Brain Mapping 1:221–234.

Herscovitch P, Markham J, Raichle ME (1983) Brain blood flow measured with intravenous $H_2{}^{15}O$. I. Theory and error analysis. J Nucl Med 24:782–789.

Jeannerod M (1984) The timing of natural prehension movements. J Mot Behav 16:235–254.

Jeannerod M (1988) Impairments of visuomotor control following

cortical lesions. The neural and behavioral organization of goal-directed movements. Oxford: Clarendon.
Jeannerod M, Marteniuk RG (1992) Functional characteristics of prehension: from data to artificial neural networks. In: Vision and motor control (Proteau L, Elliott D, eds), pp 197–232. New York: Elsevier.
Jeannerod M, Decety J, Michel F (1994) Impairment of grasping movements following a bilateral posterior parietal lesion. Neuropsychologia 32:369–380.
Kaas JH (1992) Do humans see what monkeys see? Trends Neurosci 15:1–3.
Kalaska JF, Crammond DJ (1992) Cerebral cortical mechanisms of reaching movements. Science 255:1517–1523.
Lüders H, Lesser RP, Dinner DS, Hahn JF, Salanga V, Morris HH (1985) The second sensory area in humans: evoked potential and electrical stimulation studies. Ann Neurol 17:177–184.
Luppino G, Matelli M, Camarda RM, Gallese V, Rizzolatti G (1991) Multiple representations of body movements in mesial area 6 and the adjacent cingulate cortex: an intracortical microstimulation study in the macaque monkey. J Comp Neurol 311:463–482.
Marteniuk RG, MacKenzie CL, Jeannerod M, Athenes S, Dugas C (1987) Constraints on human arm movement trajectories. Can J Psychol 41:365–378.
Marteniuk RG, Leavitt JL, MacKenzie CL, Athenes S (1990) Functional relationships between grasp and transport components in a prehension task. Hum Move Sci 9:149–176.
Mazziotta JC, Huang S-C, Phelps ME, Carson RE, MacDonald NS, Mahoney K (1985) A noninvasive positron computed tomography technique using oxygen-15-labeled water for the evaluation of neurobehavioral task batteries. J Cereb Blood Flow Metab 5:70–78.
Mesulam M-M (1985) Patterns in behavioral neuroanatomy: association areas, the limbic system, and hemispheric specialization. In: Principles of behavioral neurology (Mesulam M-M, ed), pp 1–58. Philadelphia: Davis.
Minoshima S, Koeppe RA, Mintun MA, Berger KL, Taylor SF, Frey KA, Kuhl DE (1993) Automated detection of the intercommissural line for stereotactic localization of functional brain images. J Nucl Med 34:322–329.
Mishkin M (1979) Analogous neural models for tactual and visual learning. Neuropsychologia 17:139–150.
Mitz AR, Godschalk M, Wise SP (1991) Learning-dependent neuronal activity in the premotor cortex. Activity during the acquisition of conditional motor associations. J Neurosci 11:1155–1172.
Neter J, Wasserman W, Kutner MH (1990) Applied linear statistical models. Boston: Irwin.
Ono M, Kubik S, Abernathy CD, Yasargil MG (1990) Atlas of the cerebral sulci. New York: Thieme.
Paulignan Y, MacKenzie C, Marteniuk R, Jeannerod M (1990) The coupling of arm and finger movements during prehension. Exp Brain Res 79:431–435.
Paulignan Y, MacKenzie C, Marteniuk R, Jeannerod M (1991a) Selective perturbation of visual input during prehension movements. 1. The effects of changing object position. Exp Brain Res 83:502–512.
Paulignan Y, Jeannerod M, MacKenzie C, Marteniuk R (1991b) Selective perturbation of visual input during prehension movements. 2. The effects of changing object size. Exp Brain Res 87:407–431.
Penfield W, Jasper H (1954) Epilepsy and the functional anatomy of the human brain. Boston: Little, Brown.
Petrides M, Alivisatos B, Evans AC, Meyer E (1993) Dissociation of human mid-dorsolateral from posterior dorsolateral frontal cortex in memory processing. Proc Natl Acad Sci USA 90:873–877.
Preuss TM, Goldman-Rakic PS (1989) Connections of the ventral granular frontal cortex of macaques with perisylvian premotor and somatosensory areas: anatomic evidence for somatic representation in primate frontal association cortex. J Comp Neurol 282:293–316.
Raczkowski D, Kalat JW (1980) Reliability and validity of some handedness questionnaire items. Neuropsychologia 18:213–217.
Raichle ME, Martin WRW, Herscovitch P (1983) Brain blood flow measured with intravenous $H_2{}^{15}O$. II. Implementation and validation. J Nucl Med 24:790–798.
Rizzolatti GM (1987) Functional organization of area 6. In: Motor areas of the cerebral cortex, pp 171–182. Chichester: Wiley.
Rizzolatti GM, Gentilucci L, Fogassi G, Luppino G, Matelli M, Ponzoni-Maggi S (1987) Neurons related to goal-directed motor acts in inferior area 6 of the macaque monkey. Exp Brain Res 67:220–224.
Roland PE, Skinhøj E, Lassen NA, Larsen B (1980) Different cortical areas in man in organization of voluntary movements in extrapersonal space. J Neurophysiol 43:137–150.
Rumeau C, Tzourio N, Murayama N, Peretti-Viton P, Levrier O, Joliot M, Mazoyer B, Salamon G (1994) Location of hand function in the sensorimotor cortex: MR and functional correlation. Am J Neuroradiol 15:567–572.
Sakata H, Taira M, Mine S, Murata A (1992) Hand-movement related neurons of the posterior parietal cortex of the monkey: their role in visual guidance of hand movements. In: Control of arm movement in space: neurophysiological and computational approaches (Camaniti R, Johnson PB, Burnod Y, eds), pp 185–198. Berlin: Springer.
Sergent J (1994) Brain-imaging studies of cognitive functions. Trends Neurosci 17:221–227.
Taira M, Georgopolis AP, Murata A, Sakata H (1990) Parietal cortex neurons of the monkey related to the visual guidance of hand movement. Exp Brain Res 79:155–166.
Talairach J, Tournoux P (1988) Co-planar stereotaxic atlas of the brain. New York: Thieme.
Watson JD, Myers R, Frackowiak RS, Hajnal JV, Woods RP, Mazziotta JC, Shipp S, Zeki S (1993) Area V5 of the human brain: evidence from a combined study using positron emission tomography and magnetic resonance imaging. Cereb Cortex 3:79–94.
Wise SP, Desimone R (1988) Behavioral Neurophysiology: Insights into seeing and grasping. Science 242:736–741.
Woods RP, Cherry SR, Mazziotta JC (1992) Rapid automated algorithm for aligning and reslicing PET images. J Comput Assist Tomogr 115:565–587.
Woods RP, Mazziotta JC, Cherry SR (1993a) Automated image registration. Ann Nucl Med [Suppl] 7:S70.
Woods RP, Mazziotta JC, Cherry SR (1993b) MRI-PET registration with automated algorithm. J Comput Assist Tomogr 17:536–546.
Worsley KJ, Evans AC, Marrett S, Neelin P (1992) A three-dimensional statistical analysis for CBF activation studies in human brain. J Cereb Blood Flow Metab 12:900–918.
Zeki S, Watson JDG, Lueck CJ, Friston KJ, Kennard C, Frackowiak RSJ (1991) A direct demonstration of functional specialisation in human visual cortex. J Neurosci 11:641–649.